# Physics of Propagation in Left-Handed Guided Wave Structures at Microwave and Millimeter-Wave Frequencies

Clifford M. Krowne*

*Microwave Technology Branch, Electronics Science & Technology Division, Naval Research Laboratory, Washington, D.C. 20375-5347, USA*

(Received 20 February 2003; published 3 February 2004)

A microstrip configuration is loaded with a left-handed medium substrate and studied regarding its dispersion diagrams over the microwave and millimeter-wave frequency bands for a number of different modal solutions. *Ab initio* calculations are accomplished self-consistently with a computer code using a full-wave integral equation numerical method based upon a Green's function employing appropriate boundary conditions. Bands of both propagating and evanescent behavior are discovered in some of the modes. Electromagnetic field plots in the cross-sectional dimension are made. New electric field line and magnetic circulation patterns are discovered.

DOI: 10.1103/PhysRevLett.92.053901 PACS numbers: 41.20.Jb, 84.40.–x

Tremendous interest in the last few years has been aroused with the experimental realization of macroscopic demonstrations of left-handed media (LHM), predicted or at least suggested in the literature several decades ago [1]. Attention has followed on the focusing characteristics of left-hand media, with appropriate arrangements to accomplish such behavior, as shown by the literature [2]. But no attention has been directed toward what left-handed media could accomplish in propagating devices used in integrated circuit configurations, especially with recent efforts on metamaterials. Previously, we found that modifying the anisotropic properties of the ferroelectric permittivity $\varepsilon$ [3] or ferromagnetic permeability $\mu$ [4] tensor subject to a static electric or magnetic bias field results in varying propagation behavior. Examination of the electromagnetic field distributions in these cases demonstrates the ability to modify the intensity and field line directions of the electric and magnetic fields.

In this Letter, we report on the new physics associated with altering the electromagnetic fields of guided wave propagating structures using isotropic left-handed media (scalar $\varepsilon$ and $\mu$) at microwaves and millimeter waves. As seen recently in the literature, left-handed materials, i.e., with $\mathrm{Re}[\varepsilon(\omega)] < 0$ and $\mathrm{Re}[\mu(\omega)] < 0$ simultaneously, can have wide band behavior [5], although this was not thought to be the case previously [6]. So in order to study what a left-handed substrate would do in a certain configuration, we set $\mathrm{Re}[\varepsilon(\omega)] = -\varepsilon_r$ and $\mathrm{Re}[\mu(\omega)] = -\mu_r$ where $\varepsilon_r$, $\mu_r$ = real positive constants. Sweeping the frequency over a range for these settings will yield the interaction of the guiding structure on the left-handed medium, giving the fundamental guided wave behavior.

The Green's function for the problem is a self-consistent one [7] for a driving current vector Dirac delta function applied at the guiding microstrip metal, $\mathbf{J} = j_x\delta(x - x_0)\hat{\mathbf{x}} + j_z\delta(x - x_0)\hat{\mathbf{z}}$ ($x_0 = 0$ for a centered strip). Although this Green's function is isotropic, it comes from a general spectral domain (Fourier transform) approach which is anisotropic. The Green's function is a dyadic, constructed as a $2 \times 2$ array relating tangential $x$ and $z$ components of surface current density to tangential electric field components. This Green's function is used to solve for the propagation constant. The determination of the field components is done in a second stage of processing, which in effect creates a large rectangular Green's function array, of $6 \times 2$ size in order to generate all electromagnetic field components, including those in the $y$ direction normal to the structure layers. The self-consistent problem is solved by expanding the surface currents on the guiding microstrip metal in a truncated expansion $J_x = \sum_{i=1}^{n_x} a_{xi} j_{xi}(x)$ and $J_z = \sum_{i=1}^{n_z} a_{zi} j_{zi}(x)$ and then requiring the determinant of the resulting system of equations using the Galerkin technique to be zero utilizing the moment numerical method. At this step of the problem, only the basis current functions (a complete set) need be provided and the complex propagation constant $\gamma = \alpha + j\beta$ is returned by the code. Of course, the summation limits $n_x$ and $n_z$ must be truncated at an appropriate value where convergence is acceptable.

The acquisition of the electromagnetic fields necessitates obtaining the basis function expansion coefficients $a_{xi}$ and $a_{zi}$, explicitly constructing the actual driving surface current density on the microstrip metal, finding the resulting top or bottom boundary fields, and then utilizing operators $P_{u,d}$ to pull up or down through the structure layers, generating the electric and magnetic fields in the process. The theory of $P_{u,d}$ operators is in [7] and their use in line plots in [8], the Cayley-Hamilton theorem in the Green's function for matrix exponentiation is in [9], and the eigenvalue-eigenvector theory in the determination of $P_{u,d}$ with its matrix exponentiation is found in [7]. The entire solution method uses the constraint that the vertical sidewalls of the device are perfect electric walls (perfect conductors), which can be shown to discretize the eigenvalues in the $x$ direction (top and bottom structure walls are also perfect electric walls). These are the Fourier transform variables for the spectral domain, and an infinite set of them forms a complete set

  

for the problem. Only a finite number of them are used, their maximum number being denoted by $n$.

To gain some idea of the trend of the propagation constant $\gamma = \alpha + i\beta$, a dispersion diagram is graphed in Fig. 1 ($\alpha$ is a dashed green line, $\beta$ a solid blue line) between 1 and 100 GHz for a device with air above the substrate and left-handed medium below with $\mathrm{Re}[\varepsilon(\omega)] = -\varepsilon_r = -2.5$ and $\mathrm{Re}[\mu(\omega)] = -\mu_r = -2.5$, substrate thickness $h_s = 0.5$ mm, microstrip width $w = 0.5$ mm, air region thickness $h_a = 5.0$ mm, and vertical wall separation $2b = 5.0$ mm. Also, $\mathrm{Im}[\varepsilon(\omega)] = -\varepsilon_i = 0.0$ and $\mathrm{Im}[\mu(\omega)] = -\mu_i = 0.0$ making the medium lossless (we also consider the microstrip metal lossless, although modifications for loss can be made [10]). There are two roots shown for even symmetry of the $J_z$ surface current component with respect to the $x$ axis (in plane axis). They are mirror images of each other, with the correct sign of $\alpha$ in $\gamma$ in the region of evanescence from 6.5 to 74 GHz ($\exp[-\gamma z]$ needs $\alpha > 0$ for forward propagation $z > 0$ when time dependence is $\exp[i\omega t]$ and $\beta > 0$). We identify these modes graphed as the fundamental modes since they exist even as $\omega \to 0$. An ordinary microstrip, in contrast, has a single dispersion curve (say for positive $z$ propagation) which only slowly rises with $\omega$. Thus, this structure could hold promise for new types of filters, isolators, or circulators because of an evanescent region, or backward wave devices [5] at either low or high $\omega$. Figure 1 inset shows a blowup of the previous dispersion diagram between 1–6 GHz for these fundamental modes plus the next two higher order even symmetric modes. Out of the region of evanescence, $\alpha$ goes identically to zero, producing a pure propagating mode (only $\beta \neq 0$). These dispersion diagrams were produced with $n_x = n_z = 1$ although we have found $\gamma$ solutions at selected frequencies up to $n_x = n_z = 9$, the change in numerical value being in the fourth decimal place.

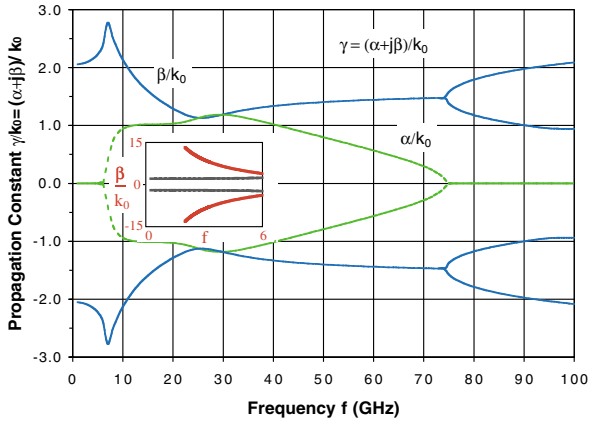


FIG. 1 (color). Complex propagation constant $\gamma$ versus frequency $f$ over the range 1–100 GHz. Fundamental modes for the microstrip configuration with a left-handed substrate. Inset: Lower end mode region 1–6 GHz.

The propagation constant was determined to be $\gamma = (0.0000, \pm 2.226\,63)$ for the fundamental mode and $(0.0000, \pm 4.9556)$ for the first higher order mode at $f = 5$ GHz in the propagating region. In the evanescent region, the fundamental mode has $\gamma = (\pm 0.9394, \pm 2.1341)$ at 10 GHz. In the millimeter-wave propagating region at 80 GHz, there are many solutions, and we list the two fundamentals and the next four higher order modes; $\gamma = (0.0000, \pm 1.7886)$, $(0.0000, \pm 1.1777)$, $(0.0000, \pm 0.902\,25)$, $(0.0000, \pm 0.873\,69)$, $(0.0000, \pm 0.696\,13)$, and $(0.0000, \pm 0.650\,65)$.

Figure 2 shows a field line plot of the electric $\mathbf{E}$ (blue) and magnetic $\mathbf{H}$ fields (red) at 5.0 GHz for the fundamental mode with the line discretization set at about 0.02 mm. Physics of the field line directions is different for structures with left-handed media than for those with only regular media. This is very clearly evidenced in Fig. 2 for the propagation case. Maxwell's electric divergence equation in integral form is

$$\oint \mathbf{D}(x, y; t) \cdot d\mathbf{s} = \iint_A q(x, y; t) da = Q(t) \qquad (1)$$

in the cross section $A$, $d\mathbf{s}$ an oriented line element (with its orientation normal to contour $S$), $da$ an area element, and $Q(t)$ the total strip charge per unit length (in the $z$-propagation direction). Since the constitutive relationship is $\mathbf{D} = \varepsilon\mathbf{E}$, (1) may be rewritten as ($S = S_{\mathrm{top}} + S_{\mathrm{LHM}}$)

$$\int_{S_{\mathrm{top}}} \varepsilon_{\mathrm{top}} \mathbf{E}(x, y; t) \cdot d\mathbf{s} + \int_{S_{\mathrm{LHM}}} \varepsilon_{\mathrm{LHM}} \mathbf{E}(x, y; t) \cdot d\mathbf{s} = Q(t). \qquad (2)$$

Taking into account that $\varepsilon_{\mathrm{LHM}} = -|\varepsilon_{\mathrm{LHM}}|$, this may be expressed as

$$\varepsilon_{\mathrm{top}} \int_{S_{\mathrm{top}}} \mathbf{E}(x, y; t) \cdot d\mathbf{s} - |\varepsilon_{\mathrm{LHM}}| \int_{S_{\mathrm{LHM}}} \mathbf{E}(x, y; t) \cdot d\mathbf{s} = Q(t). \qquad (3)$$

Supposing charge to reside on the microstrip metal as a bilayer, negative on top and positive below, contour

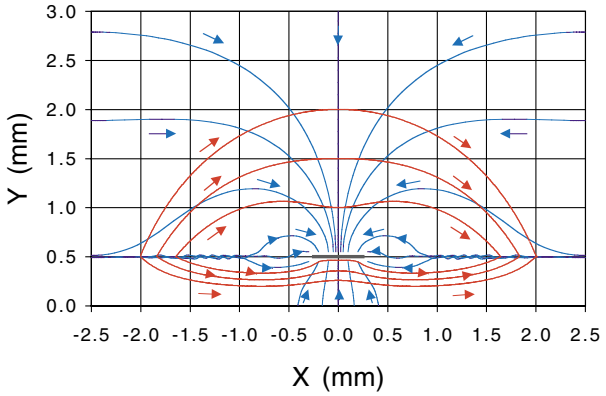


FIG. 2 (color). Electromagnetic field line plot showing electric $\mathbf{E}$ (blue) and magnetic $\mathbf{H}$ (red) fields at 5.0 GHz, in the lower propagating mode region.

contributions to the integral in (1) will oppose each other in (3) if the integral $\int_S \mathbf{E}(x, y; t) \cdot d\mathbf{s}$ keeps the same negative sign in going from above the interface to below it into the left-handed medium. This is precisely what occurs, as **E** field lines point downward above and upward below the microstrip. The enclosing surface $S$ may be imagined as a closed line encircling the microstrip, with its normal pointing outward, the direction of the differential element $d\mathbf{s}$. By extending the $S_{\text{top}}$ surface contour along the $x$ axis exactly through the center of the metal ($\mathbf{E} = 0$), making it closed, and doing the same for the $S_{\text{LHM}}$ surface contour, these integrations being opposite, form representations of the upper or lower components of the bilayer charges. The particular charge distribution seen on the metal, in terms of its top and bottom surface distributions and $x$ variation (the main contribution produces a $z$-directed symmetric "u-shaped" $J_z$), will depend on the particular mode examined.

Away from the driving currents on the microstrip metal,

$$D_{n,\text{top}} = D_{n,\text{LHM}}; \tag{4a}$$

$$\mathbf{n} \times [\mathbf{E}_{\text{top}} - \mathbf{E}_{\text{LHM}}] = 0. \tag{4b}$$

Looking at the electric field lines, and using the constitutive relationship, (4a) and (4b) can be recast as

$$\varepsilon_{\text{top}} E_{n,\text{top}} = \varepsilon_{\text{LHM}} E_{n,\text{LHM}}; \tag{5a}$$

$$E_{\text{tan,top}} = E_{\text{tan,LHM}}. \tag{5b}$$

Inserting $\varepsilon_{\text{LHM}} = -|\varepsilon_{\text{LHM}}|$ into (4a) gives

$$\varepsilon_{\text{top}} E_{n,\text{top}} = -|\varepsilon_{\text{LHM}}| E_{n,\text{LHM}}. \tag{6}$$

Invoking (5b) and (6) at the interface for $b > |x| > w/2$ means that the electric field lines above and below the interface must both point toward or away from the interface, which is seen in Fig. 3.

Maxwell's magnetic curl equation in integral form is

$$\oint_L \mathbf{H}(x, y; t) \cdot d\mathbf{l} = \iint_A \mathbf{J}(x, y; t) \cdot d\mathbf{a} = I(t), \tag{7}$$

where the current density **J** is made up of displacement, volumetric, and microstrip surface currents. The line integral on the left may be broken down into its pieces such as (2) above, giving

$$\int_{L_{\text{top}}} \mathbf{H}(x, y; t) \cdot d\mathbf{l} + \int_{L_{\text{LHM}}} \mathbf{H}(x, y; t) \cdot d\mathbf{l} = I(t). \tag{8}$$

Using the constitutive relationship $\mathbf{B} = \mu\mathbf{H}$ and $\mu_{\text{LHM}} = -|\mu_{\text{LHM}}|$,

$$\frac{1}{\mu_{\text{top}}} \int_{L_{\text{top}}} \mathbf{B}(x, y; t) \cdot d\mathbf{l} - \frac{1}{|\mu_{\text{LHM}}|} \int_{L_{\text{LHM}}} \mathbf{B}(x, y; t) \cdot d\mathbf{l} = I(t). \tag{9}$$

This has a similar form to (3), and we may wonder if here as well the contour pieces have some relationship to each other in terms of their polarity. They do and this is discovered if we examine the continuity condition for magnetic field **B** at the ordinary dielectric/left-handed medium interface located at, say, some $x < 0$ off of the microstrip metal, that is for $b < x < -w/2$. Normal **B** field components must be continuous across the interface, whereas tangential **H** field components must be

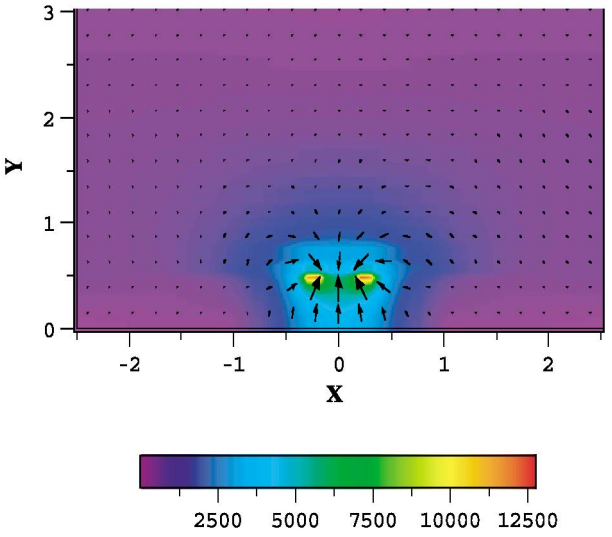


FIG. 3 (color). Electromagnetic field color plot showing electric field magnitude $E$ (color variation) with an overlaid vector field **E** (black arrows) at 5.0 GHz.

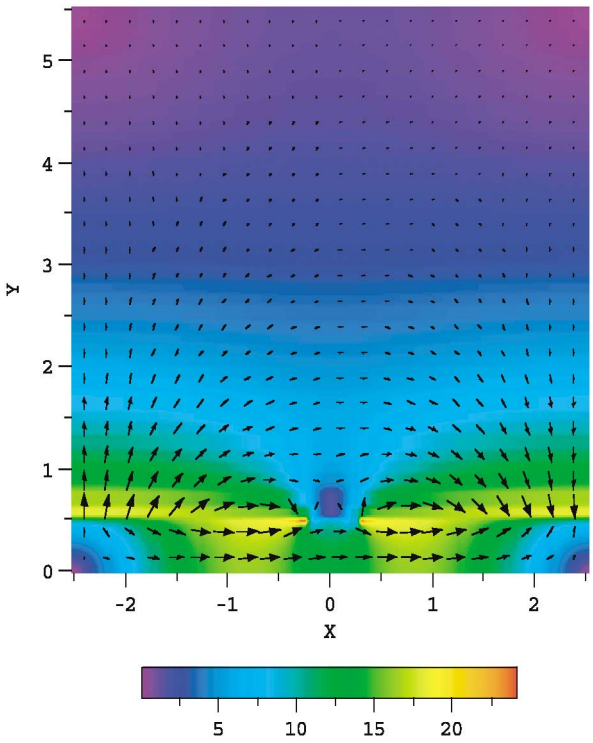


FIG. 4 (color). Electromagnetic field color plot showing magnetic field magnitude $H$ (color variation) with an overlaid vector field **H** (black arrows) at 5.0 GHz.

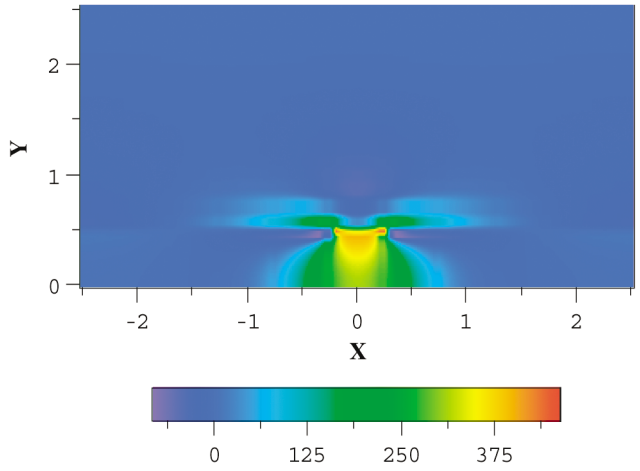


FIG. 5 (color). Electromagnetic color plot showing the Poynting vector $P_{\text{guide}}$ (color variation) in the guiding $z$ direction at 5.0 GHz (actually shows $-P_{\text{guide}}$ in reference to Figs. 2–4).

discontinuous by the surface current $\mathbf{J}_s$. Thus,

$$B_{n,\text{top}} = B_{n,\text{LHM}}; \tag{10a}$$

$$\mathbf{n} \times [\mathbf{H}_{\text{top}} - \mathbf{H}_{\text{LHM}}] = \mathbf{J}_s. \tag{10b}$$

Looking at the magnetic field lines away from the microstrip, $\mathbf{J}_s = 0$, and again using the constitutive relationship, (10a) and (10b) can be recast as

$$\mu_{\text{top}} H_{n,\text{top}} = \mu_{\text{LHM}} H_{n,\text{LHM}}; \tag{11a}$$

$$H_{\text{tan,top}} = H_{\text{tan,LHM}}. \tag{11b}$$

Inserting $\mu_{\text{LHM}} = -|\mu_{\text{LHM}}|$ into (11a) gives

$$\mu_{\text{top}} H_{n,\text{top}} = -|\mu_{\text{LHM}}| H_{n,\text{LHM}}. \tag{12}$$

Applying (11b) and (12) at the interface for $b > |x| > w/2$ means that the magnetic field lines above and below the interface must both point toward or away from the interface. This is indeed the case as seen in Fig. 2. And it is found that integral $\int_L \mathbf{B}(x, y; t) \cdot d\boldsymbol{l}$ holds the same positive sign in going from above the interface to below it into the left-handed medium.

A different visualization technique is provided in Figs. 3 and 4 to complete the field assessment where we have produced color variation of the magnitude of the electric $E = \text{sqrt}[\sum_{i=1}^{3} E_i^2]$ and magnetic $H = \text{sqrt}[\sum_{i=1}^{3} H_i^2]$ fields with overlays of the $\mathbf{E}$ and $\mathbf{H}$ vectors with arrows sized according to magnitude. Figures 3 and 4 are produced from a grid of 8372 points stored in a 1 MB file. Finally, power flow is given by the Poynting vector $\mathbf{P} = \mathbf{E} \times \mathbf{H}$. Assessment of $\mathbf{P}$ using only the cross-sectional fields yields information about the propagation in the guide direction, $\hat{z}$, so $\mathbf{P}_{\text{guide}} = \mathbf{E}_t \times \mathbf{H}_t = P_{\text{guide}} \hat{z}$. Figure 5 gives $P_{\text{guide}}$ in a distribution which shows that sign reversals occur, possibly caused by the coalescence of two modal behaviors. Immediately to either side of the interface (off of the strip metal), sign reversal is consistent with a RHM (right-handed medium) to LHM change. Of course, total power $P_T$ down the guiding structure is given by $P_{Tz} = \oint\!\!\oint_S \mathbf{P} \cdot d\mathbf{a} = \oint\!\!\oint_S \mathbf{E} \times \mathbf{H} \cdot d\mathbf{a}$.

Another important question is causality. Although the calculations presented here and in [11] have taken the LHM substrate loss as zero, we have performed additional simulations with loss in the LHM by letting $\varepsilon_i = -0.0025$ ($\text{Im}[\varepsilon(\omega)] = -\varepsilon_i > 0$) at $f = 5\,\text{GHz}$. This leads to waves which decay in either the $\pm z$ directions for, respectively, $\alpha, \beta > 0$ or $\alpha, \beta < 0$, preserving causality. Change of the $\gamma$ eigenvalue due to the added loss is small, with no apparent change in $\beta$, $\alpha/k_0$ rising from 0 to 0.002 062. The current expansion coefficient change is from $[a_{x1}, a_{x1}] = [(0, -1.2043 \times 10^{-3}), (1, 0)]$ to $[(-4.7273 \times 10^{-7}, -1.2043 \times 10^{-3}), (1, 0)]$, and the field components change in the fourth decimal place or higher, causing no visual alteration of the field distributions.

*Email address: krowne@chrisco.nrl.navy.mil

[1] V. G. Veselago, Sov. Phys. Usp. **10**, 509 (1968).
[2] D. R. Smith, W. Padilla, D. Vier, S. Nemat-Nasser, and S. Schultz, Phys. Rev. Lett. **84**, 4184 (2000); D. R. Smith and N. Kroll, Phys. Rev. Lett. **85**, 2933 (2000); J. B. Pendry, Phys. Rev. Lett. **85**, 3966 (2000); R. A. Shelby, D. R. Smith, and S. Schultz, Science **292**, 77 (2001); R. A. Shelby, D. R. Smith, S. C. Nemat-Nasser, and S. Schultz, Appl. Phys. Lett. **78**, 489 (2001); P. M. Valanju, R. M. Walser, and A. P. Valanju, Phys. Rev. Lett. **88**, 187401 (2002); N. Garcia and M. Nieto-Vesperinas, Phys. Rev. Lett. **88**, 207403 (2002).
[3] C. M. Krowne, Microwave Opt. Tech. Lett. **28**, 63 (2001). The $zy$ element of $\bar{\bar{\varepsilon}}'$ should be 0 in (30). C. M. Krowne, M. Daniel, S.W. Kirchoefer, and J. M. Pond, IEEE Trans. Microwave Theory Tech. **50**, 537 (2002); C. M. Krowne, Microwave Opt. Tech. Lett. **17**, 213 (1998).
[4] C. M. Krowne, Proc. SPIE-Int. Soc. Opt. Eng. **4097**, 70 (2000). The $zy$ element of $\bar{\bar{\mu}}'$ should be 0 in (43).
[5] A. K. Iyer and G.V. Eleftheriades, IEEE MTT-S Int. Microwave Symp. Digest, p. 222 (2002). See also papers in IEEE MTT-S Int. Microwave Symp. Digest, in Neg. Refract. Index. Mat. & Appl., pp. 187–206; Neg. Index Mat. & Micro. Appli., pp. 309–332 (2003).
[6] J. B. Pendry, A. J. Holden, W. J. Stewart, and I. Youngs, Phys. Rev. Lett. **76**, 4773 (1996); J. B. Pendry, A. J. Holden, D. J. Robbins, and W. J. Stewart, J. Phys. Condens. Matter **10**, 4785 (1998); IEEE Trans. Microwave Theory Tech. **47**, 2075 (1999).
[7] C. M. Krowne, IEEE Trans. Microwave Theory Tech. **32**, 1617 (1984).
[8] A. A. Mostafa, C. M. Krowne, K. A. Zaki, and S. Tantawi, J. Electromagn. Waves Appl. **5**, 577 (1991).
[9] A. A. Mostafa, C. M. Krowne, and K. A. Zaki, IEEE Trans. Microwave Theory Tech. **35**, 1399 (1987).
[10] C. M. Krowne, IEEE Trans. Microwave Theory Tech. **50**, 112 (2002). In (69), the numerator should read $1 + j$, not 1. In (70), factors 1, 2 and 1 are associated with (61), (64), and (65).
[11] C. M. Krowne, Bull. Am. Phys. Soc. **48**, Pt. 1, 580 (2003).